Published in final edited form as:
Drug Metab Dispos. 2007 June ; 35(6): 973–980.

A Functional Genetic Polymorphism on Human Carbonyl Reductase 1 (*CBR1* V88I) Impacts on Catalytic Activity and NADPH Binding Affinity

Vanessa Gonzalez-Covarrubias, **Debashis Ghosh**, **Sukhwinder S. Lakhman**, **Lakshmi Pendyala**, and **Javier G. Blanco**

Department of Pharmaceutical Sciences, The State University of New York at Buffalo, Buffalo, New York (V.G.-C., S.S.L, J.G.B.); and Department of Structural Biology, Hauptman-Woodward Medical Research Institute and Department of Pharmacology and Therapeutics (D.G.), and Department of Medicine, Roswell Park Cancer Institute, Buffalo, New York (L.P.)

Abstract

Human carbonyl reductase 1 (CBR1) metabolizes endogenous and xenobiotic substrates such as the fever mediator, prostaglandin E2 (PGE_2), and the anticancer anthracycline drug, daunorubicin. We screened 33 CBR1 full-length cDNA samples from white and black liver donors and performed database analyses to identify genetic determinants of CBR1 activity. We pinpointed a single nucleotide polymorphism on *CBR1* (*CBR1* V88I) that encodes for a valine-to-isoleucine substitution for further characterization. We detected the *CBR1* V88I polymorphism in DNA samples from individuals with African ancestry ($p = 0.986$, $q = 0.014$). Kinetic studies revealed that the CBR1 V88 and CBR1 I88 isoforms have different maximal velocities for daunorubicin (V_{max} CBR1 V88, 181 ± 13 versus V_{max} CBR1 I88, 121 ± 12 nmol/min · mg, $p < 0.05$) and PGE_2 (V_{max} CBR1 V88, 53 ± 7 versus V_{max} CBR1 I88, 35 ± 4 nmol/min · mg, $p < 0.01$). Concomitantly, CBR1 V88 produced higher levels of the cardiotoxic metabolite daunorubicinol compared with CBR1 I88 (1.7-fold, $p < 0.0001$). Inhibition studies demonstrated that CBR1 V88 and CBR1 I88 are distinctively inhibited by the flavonoid, rutin (IC_{50} CBR1 V88, 54.0 ± 0.4 μM versus IC_{50} CBR1 I88, 15.0 ± 0.1 μM, $p < 0.001$). Furthermore, isothermal titration calorimetry analyses together with molecular modeling studies showed that *CBR1* V88I results in CBR1 isoforms with different binding affinities for the cofactor NADPH (K_d CBR1 V88, 6.3 ± 0.6 μM versus K_d CBR1 I88, 3.8 ± 0.5 μM). These studies characterize the first functional genetic determinant of CBR1 activity toward relevant physiological and pharmacological substrates.

Human carbonyl reductase 1 (CBR1) is a monomeric cytosolic enzyme that catalyzes the two-electron reduction of biologically and pharmacologically active substrates by using NADPH as cofactor (Forrest and Gonzalez, 2000). For example, CBR1 converts the potent fever mediator prostaglandin E_2 (PGE_2) into the less active metabolite $PGF_{2\alpha}$. Recent studies have shown that the transcription of CBR1 in lung and liver is down-regulated to suppress the catabolism of PGE_2 during the course of the febrile response (Ivanov et al., 2003; Ivanov and Romanovsky, 2004). CBR1 also plays a predominant role in the metabolism of the anticancer anthracyclines doxorubicin and daunorubicin by catalyzing the formation of their corresponding C-13 alcohol metabolites (doxorubicinol and daunorubicinol). Anthracycline C-13 alcohol metabolites circulate in plasma, have half-lives similar to those of the parent compounds, and are devoid of significant tumor cell-killing activity. The use of anthracyclines

Address correspondence to: Dr. Javier G. Blanco, Department of Pharmaceutical Sciences, The State University of New York at Buffalo, 545 Cooke Hall, Buffalo, NY 14260-1200. E-mail: jgblanco@buffalo.edu.

Article, publication date, and citation information can be found at http://dmd.aspetjournals.org.

for cancer treatment is hampered by the development of clinical cardiotoxicity in some patients (Wouters et al., 2005). The pathogenesis of anthracycline-related cardiotoxicity is complex and appears to be mediated by a combination of oxidative stress and intracardiac metabolic perturbations induced by C-13 anthracycline alcohol metabolites (Minotti et al., 2004). In human myocardium, cytosolic carbonyl reductases (CBRs), and aldo/keto reductases catalyze the two-electron reduction of the anthracycline side chain C-13 carbonyl group to form cardiotoxic alcohol metabolites (e.g., doxorubicinol, daunorubicinol). CBR activity is the main source of quinone detoxification in humans, and biochemical studies showed that aldo/keto reductases have 7- to 18-fold lower catalytic efficiencies (V_{max}/K_m) for the reduction of anthracycline substrates than CBRs (Wermuth et al., 1986; Ohara et al., 1995; Rosemond and Walsh, 2004; Covarrubias et al., 2006). The key role of CBR1 during the pathogenesis of anthracycline-related cardiotoxicity has been established in biochemical studies and in experiments with murine models (Mordente et al., 2001). Mice over-expressing human *CBR1* in heart showed high intracardiac levels of doxorubicinol and increased signs of myocardial damage after doxorubicin administration (Forrest et al., 2000). Conversely, mice with a null allele of *Cbr1* (*Cbr1*+/−) treated with doxorubicin showed low plasmatic levels of doxorubicinol and significantly lower incidence of anthracycline-related cardiotoxicity compared with animals with two active *Cbr1* alleles (*Cbr1*+/+) (Olson et al., 2003).

Carbonyl reductase activity varies widely among individuals and may contribute to the unpredictable pharmacodynamics of CBR1 drug substrates. We documented wide ranges of hepatic CBR activities by using the prototypical quinone substrate menadione in cytosols from white (range, <0.1–28.0 nmol/min · mg) and black donors (range, 4.1–21.5 nmol/min · mg) (Covarrubias et al., 2006). To the best of our knowledge, the potential contribution of genetic polymorphisms on *CBR1* to variable CBR activity has not yet been explored. Consequently, the aim of this study was to identify and characterize the functional impact of single nucleotide polymorphisms (SNPs) on the coding region of *CBR1*. Therefore, we first sequenced CBR1 full-length cDNA samples from liver donors (13 blacks and 20 whites) and performed SNP database analyses to identify SNPs in the coding region of *CBR1*. We pinpointed a SNP on *CBR1* that results in a valine-to-isoleucine substitution at position 88 (*CBR1* V88I). Next, we investigated the presence of the *CBR1* V88I polymorphism in human DNA variation panels, and we characterized the functional properties of the resulting CBR1 V88 and CBR1 I88 protein isoforms. Kinetic analyses with prototypical CBR1 substrates (e.g., PGE_2, and daunorubicin) together with data from isothermal titration calorimetry experiments demonstrate that CBR1 V88 and CBR1 I88 have distinctive functional properties. Furthermore, we discuss the impact of *CBR1* V88I in light of the recently reported X-ray crystal structure of human CBR1 (Tanaka et al., 2005). Our findings document the first genetic determinant of human CBR1 activity toward substrates of physiological and pharmacological relevance.

Materials and Methods

Human DNA and RNA Samples

Human DNA variation panels were obtained from the Coriell Institute for Medical Research (Camden, NJ). Each panel contained DNA samples from individuals representing the following groups: Mexican, South American (Andes region), Chinese, Indo-Pakistani, Japanese, Southeast Asian (excluding Japanese and Chinese), Middle Eastern, Pacific, North American (African ancestry), North American (European ancestry), African (north of the Sahara), and African (south of the Sahara). Human liver RNA samples (n = 33) were provided by the Liver Tissue Procurement and Distribution System (University of Minnesota Department of Pediatrics, Gastroenterology and Nutrition, Minneapolis, MN; National Institutes of Health Contract N01-DK-9-2310) and by the Cooperative Human Tissue Network (http://www.chtn.ims.nci.nih.gov/), respectively.

Sequencing of CBR1 Full-Length cDNA Samples

PCR amplification of CBR1 full-length cDNA followed by SNP detection by direct sequencing analysis was used to investigate genetic polymorphisms in the coding region of *CBR1* (Nickerson et al., 1997). CBR1 full-length cDNA was synthesized from 1 μg of total liver RNA by using Superscript (Invitrogen, Carlsbad, CA) and oligo(dT)$_{12–18}$ primers. PCR amplification primers located at the 5′- and 3′-untranslated regions were designed with PRIMER3 (http://frodo.wi.mit.edu/cgi-bin/primer3/primer3_www.cgi), and their sequence homologies were analyzed by BLAST (http://www.ncbi.nlm.nih.gov/blast/). Primers were as follows: forward 5′-TTCTCCACGCAGGTGTTC-3′, and reverse 5′-GCATCAGAGGAAATCACAAAAG-3′. One microliter of the cDNA conversion mixture was amplified by using the Expand Long Template PCR system with buffer 1 (Roche Diagnostics, Indianapolis, IN). PCR amplification conditions were 95°C for 2 min; 45 cycles of 95°C for 35 s, 57.5°C for 40 s, and 68°C for 70 s; and final extension at 70°C for 10 min. Aliquots of PCR products were visualized by UV light after size-fractionation in 1.0% agarose gels supplemented with ethidium bromide (0.5 μg/ml). All samples presented a unique 1077-bp band.

PCR products were treated with ExoSAP-IT (U.S. Biochemical Corp., Cleveland, OH) and purified with PCR cleanup kits (QIAGEN, Valencia, CA). Purified products were sequenced with both forward and reverse PCR primers, and with the internal sequencing primer 5′-TCTGGTGCACTCCCTTCTTT-3′, by using the dye-terminator method in an ABI PRISM 3130 XL Genetic Analyzer (Applied Biosystems, Foster City, CA). The resultant trace files were assembled and analyzed with PolyPhred (http://lpgws.nci.nih.gov/perl/snp/snp_cgi.pl), and with Vector NTI (Invitrogen). PolyPhred detects the presence of single nucleotide substitutions using fluorescence sequencing of PCR products. To be considered a true variant, the SNPs were confirmed with forward and reverse primers.

CBR1 V88I Genotyping

The *CBR1* V88I polymorphism (rs1143663) was investigated by using two genotyping techniques. The first approach utilized the TaqMan technology with specific fluorescent probes labeled with the fluorochromes 5-carboxyfluorescein (FAM) and VIC to discriminate the G and the A alleles, respectively (Applied Biosystems, Assays-by-Design). Genotyping reactions were performed according to the manufacturer's protocol in a Bio-Rad IQ5 thermal cycler (Bio-Rad, Hercules, CA). Genotyping controls for each allele combination were prepared by diluting plasmid DNA (30 ng/μl) containing the *CBR1* V88 insert (G/G genotype), the *CBR1* I88 insert (A/A genotype), and a mixture (1:1) of *CBR1* V88 plus *CBR1* I88 inserts (G/A genotype), respectively (see further details under *Cloning and Expression of CBR1 V88 and CBR1 I88*). The second *CBR1* V88I genotyping approach involved PCR amplification of a fragment of *CBR1* (183 bp) followed by SNP detection by direct sequencing analysis. In brief, 50 ng of genomic DNA were amplified using 2.5 units of Amplitaq Gold DNA polymerase (Applied Bio-systems) with the following primers: 5′-CTTCCACCAGCTGGACATC-3′ (forward) and 5′-CCAGTGCATCGGTTCTTCTT-3′ (reverse). PCR amplification conditions were 92°C for 2 min, followed by 45 cycles of 92°C for 30 s, 57°C for 30 s, and 72°C for 70 s. PCR products were verified by agarose gel electrophoresis (2.0%). PCR products were treated with ExoSAP-IT (U.S. Biochemical Corp.), purified with QIAquick kits (QIAGEN), and sequenced with forward and reverse PCR primers by using the dye-terminator method. The resultant trace files were analyzed as described above.

Cloning and Expression of *CBR1* V88 and *CBR1* I88

CBR1 V88 full-length cDNA was obtained by reverse transcription-PCR using liver RNA from a donor with *CBR1* V88I homozygous G/G genotype as template. Total liver RNA (1 μg) was reverse-transcribed by using Superscript (Invitrogen) and primers. The resulting cDNA was

amplified with the oligo(dT)$_{12–18}$ Expand Long Template PCR System (Roche Diagnostics) with the following primers: 5′-CATATGTCGTGGCATCCATGTAGC-3′ (forward), and 5′-CTCGAGTCACCACTGTTCAACTCTCTTCTC-3′ (reverse). The PCR product was purified and cloned into a pET28a expression vector (EMD, Novagen, San Diego, CA). The insert was fully sequenced with vector- and insert-specific primers to confirm its identity and the absence of mutations. The pET28a *CBR1* V88 clone was used as template to generate the variant *CBR1* I88 insert by site-directed mutagenesis (QuikChange; Stratagene, La Jolla, CA) with the following primers: 5′-GGCCTGGACGTGCTGATCAACAACGCGGGCATCG-3′ (forward), and 5′-CGATGCCCGCGTTGTTGATCAGCACGTCCAGGCC-3′ (reverse). The amplicon was treated with DpnI, and the resultant fragment was used to transform XL-10 Gold Ultra-competent cells (Stratagene). Cells were cultured and selected with kanamycin (30 μg/ml). After selection, plasmid DNA was extracted and purified using QIAprep Spin Miniprep kits (QIAGEN). The integrity of the *CBR1* I88 construct was confirmed by sequencing. *CBR1* V88 and *CBR1* I88 constructs were transfected into *Escherichia coli* BL21 (DE3)-competent cells. Cells were plated on Luria-Bertani broth agar supplemented with kanamycin (30 μg/ml) for selection. Colonies were randomly picked and cultured overnight at 37°C in 100 ml of Luria-Bertani broth with kanamycin (15 μg/ml). Cultures were expanded to 1 liter and induced with isopropyl-β-D-thiogalactoside (1 mM). *E. coli* cells were pelleted and lysed in buffer containing 50 mM sodium phosphate, 10 mM imidazole, 300 mM NaCl, 1 mM dithiothreitol, 1 mM phenylmethylsulfonyl fluoride, 1 mM pepstatin, and 10 μM NADPH. Lysates were supplemented with lysozyme (1 mg/ml), DNase I (5 μg/ml), and ribonuclease (10 μg/ml). Lysates were sonicated and centrifuged for 30 min at 4°C (25,000*g*). The resulting supernatants were filtered through a 0.45-μm polyvinylidene fluoride membrane (Millipore, Billerica, MA) and transferred to vials equilibrated with nickel nitrilotriacetic acid His-Bind Resin (Superflow; EMD, Novagen). CBR1 V88 and CBR1 I88 proteins were eluted in buffer containing 50 mM sodium phosphate, pH 8.0, 300 mM NaCl, 250 mM imidazole, and 1 mM dithiothreitol. Proteins were extensively dialyzed for 48 h in phosphate-buffered saline at 4°C with two buffer changes (4 liters each). After dialysis, proteins were aliquoted and stored at −80°C.

Western Blotting

Recombinant CBR1 V88 and CBR1 I88 proteins were electrophoresed on 4 to 20% precast polyacrylamide gels (Pierce, Rockford, IL) and transferred to Hybond polyvinylidene difluoride membranes (GE Healthcare, Chalfont St. Giles, Buckinghamshire, UK). Membranes were first incubated with a polyclonal anti-human CBR1 antibody (1:1000 dilution; Abcam Inc., Cambridge, MA), followed by incubation with a secondary rabbit anti-goat IgG antibody conjugated with horseradish peroxidase (1:10,000 dilution; Sigma-Aldrich, St. Louis, MO). Immunoreactive bands were visualized with the ECL Plus Western blotting detection system (Amersham Biosciences) by using a ChemiDoc XRS gel documentation system equipped with Quantity One software (Bio-Rad).

Kinetic Analysis

CBR1 V88 and CBR1 I88 enzymatic activities were measured by recording the rate of oxidation of the NADPH cofactor at 340 nm (NADPH molar absorption coefficient, 6220 M^{-1} cm^{-1}) (Wermuth, 1981; Bohren et al., 1987; Lakhman et al., 2005). Experiments were performed in a Cary-Varian Bio 300 UV-visible spectrophotometer equipped with thermal control and proprietary software for enzyme kinetics analysis (Varian, Walnut Creek, CA). Reactions were incubated at 37°C and monitored for 3 min at an acquisition rate of 5 readings/s (900 readings). Assay mixtures (1.0 ml) contained 200 μM NADPH (Sigma-Aldrich), 100 mM potassium phosphate buffer (pH 7.4), CBR1 enzyme (1 mg/ml), and one of the following substrates: menadione (20–500 μM; Sigma-Aldrich), daunorubicin (20–650 μM; Sigma-Aldrich), or PGE_2 (40–2000 μM; Cayman Chemical, Ann Arbor, MI). The kinetic constants

of the cofactor were determined by recording activities with different NADPH concentrations (range, 10–200 μM) and with menadione at a fixed concentration of 250 μM. Enzymatic velocities (V_0) were automatically calculated by linear regression of the $\Delta_{abs}/\Delta_{time}$ points. CBR1 protein concentrations were determined by recording the absorbance at 280 nm (molar extinction coefficient, 21,500 M^{-1} cm^{-1}; http://us.expasy.org/). Enzyme kinetic parameters (K_m and V_{max}) were calculated by nonlinear regression analysis using a one-site binding model. Kinetic and statistical analyses were performed with GraphPad Prism (version 4.03; GraphPad Software Inc., San Diego, CA). CBR1 V88 and CBR1 I88 kinetic parameters were compared by using GraphPad's built-in algorithm based on the *F*-test. Statistical results were further confirmed by performing unpaired Student's *t* tests with Excel XP 2003 (Microsoft, Redmond, WA). Both statistical approaches resulted in essentially identical *p* values. Differences between means were considered to be significant at $p < 0.05$.

Daunorubicinol Quantification

The amount of daunorubicinol synthesized by CBR1 V88 and CBR1 I88 was quantified by HPLC analysis (Cowens et al., 1993). CBR1 V88 and CBR1 I88 incubation mixtures (1.0 ml) contained potassium phosphate buffer (pH 7.4, 100 mM), enzyme (1 mg/ml), NADPH (200 μM), and daunorubicin (125–500 μM). Mixtures were incubated for 30 min at 37°C, and reactions were stopped by placing samples on ice. Samples were stored at −80°C until HPLC analysis. Samples were diluted with 150 μl of ammonium formate buffer (16 mM, pH 4.0) and directly injected (25 μl) into a Waters HPLC system (Waters, Milford, MA), consisting of an M600 pump, an M717Plus autosampler, and an M474 scanning fluorescence detector with excitation and emission wavelengths set at 490 and 590 nm, respectively. Separation was performed on a reverse phase column (C8, 5 μm, 150 mm; Alltech Associates, Deerfield, IL), with a mobile phase gradient of ammonium formate and tetrahydrofuran. Doxorubicin was used as internal standard. Calibration curves with authentic daunorubicin and doxorubicin standards (0.5–20 μg/ml) were run for each determination. Daunorubicinol/internal standard ratios of the peak areas were used for quantification. For the lack of daunorubicinol standard, the daunorubicinol peak was quantified in daunorubicin equivalents. The capacity factors (K') for doxorubicin, daunorubicinol, and doxorubicinol were calculated from chromatograms by using the formula: $K' = (TA - To)/To$, where TA is the retention time of the analyte and To is the retention time of nonretained compounds. K' values were 6.6 (doxorubicin), 6.9 (daunorubicinol), and 7.8 (doxorubicinol), with resolution values of ~1 (doxorubicin), 2.1 (daunorubicinol), and 2.7 (doxorubicinol), respectively.

CBR1 V88 and *CBR1* I88 Inhibition Studies

CBR1 V88 and CBR1 I88 activities were inhibited with the flavonoid rutin (Sigma-Aldrich) in the presence of the substrate menadione (Wermuth et al., 1986; Covarrubias et al., 2006). Assay mixtures (1.0 ml) contained 200 μM NADPH, 100 mM potassium phosphate buffer (pH 7.4), CBR1 enzyme (1 mg/ml), 40 μM menadione, and rutin (5–300 μM). The concentration of rutin required to inhibit CBR1 activity by 50% (IC_{50}) was calculated by nonlinear regression analysis using a one-site model with GraphPad Prism 4.

CBR1 V88 and CBR1 I88 Thermolability

The thermolability of both CBR1 isoforms was assessed by incubating protein aliquots (1 mg/ml) in phosphate buffer (pH 7.4, 100 mM), for 5 min at the following temperatures: 46°C, 50°C, and 60°C (Weisberg et al., 2001). Control reaction mixtures were incubated at 37°C for 5 min. Incubations were performed in an Isotemp 125D dry block (Fisher Scientific Co., Pittsburgh, PA) with digital temperature control. After incubation, protein aliquots were immediately transferred to ice. CBR1 activities were assayed as described above by using menadione (200 μM) and daunorubicin (500 μM) as substrates.

Determination of CBR1 V88 and CBR1 I88 NADPH Binding Affinities

The NADPH binding affinities of CBR1 V88I and CBR1 I88 were measured by isothermal titration calorimetry using a MicroCal microcalorimeter equipped with the VP Viewer 2000 Origin software (version 7SR2.V7; MicroCal, Northampton, MA). Freshly expressed and purified CBR1 isoforms were extensively dialyzed in phosphate-buffered saline solution (PBS, pH 7.2) and Tris (2-carboxyethyl)-phosphine (1 mM) up to a final concentration of 20 to 40 μM. Protein samples were degassed and added to the sample cell. PBS was added to the reference cell, and both cells were allowed to reach a stable temperature of 30.0°C. CBR1 isoforms were titrated with the NADPH cofactor (200 μM) and with PBS to subtract for heat dilution (Pey and Martinez, 2005). Titration experiments were performed at 30.0°C with a stirring rate of 300 rpm. A total of 29 NADPH aliquots were injected (10 μl/injection) to the sample cell at 300-s intervals. Changes in heat due to enzyme-cofactor binding were automatically recorded and plotted as kcal/mol of ligand versus ligand/enzyme molar ratio. The binding affinities (K_a), dissociation constants ($K_d = 1/K_a$), enthalpies (ΔH), entropies (ΔS), and Gibbs' free energies (ΔG) were calculated by nonlinear regression analysis using a one-site binding model.

Docking and Modeling Analysis

The Molecular Operating Environment (MOE 2005.08; Chemical Computing Group, Montreal, QC, Canada) software package was used for substrate docking and modeling analysis. The *site finder* option of MOE automatically and correctly delineated the active site. Default parameters including partial charges for amino acids and ligands were turned on, and full conformational searches for the substrate PGE_2 were carried out. The pose with the best score was selected as the model for the docked substrate. To account for conformational flexibility of the active site pocket, the complex was energy minimized by restrained minimization within 9 Å of the substrate molecule. In addition, energies of the ternary CBR1-PGE_2 complexes with V88 and I88 side chains were also minimized by imposing default positional restraints on atoms within 9 Å of the cofactor atoms and fixing all atomic positions outside. PyMOL routines were used for analysis and illustrations (PyMOL Molecular Graphics System; DeLano Scientific LLC, Palo Alto, CA. http://www.pymol.org).

Results

SNPs in the Coding Region of Human *CBR1*

To identify common polymorphisms in the coding region of *CBR1*, we first screened 33 full-length cDNA samples isolated from liver donors (13 black and 20 white). The statistical power resulting from both sample sizes was adequate to detect polymorphic alleles with frequencies ≥5% ($power_{whites} \approx 0.96$, and $power_{blacks} \approx 0.85$) (Kruglyak and Nickerson, 2001). We found no common *CBR1* SNPs in cDNA samples from black donors, and we detected three synonymous *CBR1* SNPs in samples from white donors (Table 1). In whites, *CBR1* synonymous SNPs were present in 5% (V231V) and in 20% (L73L, A209A) of the samples, respectively. Genotyping data from the public dbSNP database (built 126) showed a total of nine SNPs in the coding region of *CBR1* (exon 1, four SNPs; and exon 3, five SNPs), including the synonymous SNPs V231V, L73L, and A209A. Interestingly, the dbSNP database showed only one nonsynonymous SNP on *CBR1*. The SNP is located in exon 1 (contig position, 23104545) and encodes for a valine-to-isoleucine substitution at position 88 of the amino acidic chain (*CBR1* V88I, rs:1143663). Therefore, we sought to confirm the existence of the *CBR1* V88I polymorphism by analyzing 12 human DNA variation panels representing population groups with distinctive geographical ancestries. We analyzed 211 DNA samples (422 alleles) by using a validated real-time PCR assay for *CBR1* V88I genotyping, and we confirmed the presence of the variant allele (A) by direct sequencing (Fig. 1, A and B). We detected the *CBR1* V88I polymorphism in the DNA panel representing individuals from the United States

with African ancestry (Table 2). *CBR1* V88I genotype distribution in the U.S.-African ancestry panel was as follows: 97.1% were homozygous for the G allele (G/G) and 2.9% were heterozygous (G/A). Allele distributions were in Hardy-Weinberg equilibrium (chi square test, $p = 0.93$; Table 2). Our observations were in agreement with the *CBR1* V88I allele frequencies reported in dbSNP for a panel of 24 DNA samples representing individuals from the United States with African ancestry ($p = 0.979$, $q = 0.021$).

Kinetic Characterization of CBR1 V88 and CBR1 I88

To evaluate the functional impact of the *CBR1* V88I polymorphism, we purified the recombinant CBR1 V88 and CBR1 I88 protein isoforms. Both isoforms appeared as discrete ~32-kDa bands after immunoblotting analysis with anti-human CBR1 antibody (Fig. 1C). We analyzed CBR1 V88 and CBR1 I88 kinetic activities by using the prototypical substrates menadione, PGE_2, and daunorubicin. CBR1 V88 and CBR1 I88 displayed typical one-site Michaelis-Menten kinetics for the three substrates. Kinetic comparisons with the quinone menadione demonstrated a slightly higher K_m value for CBR1 I88 compared with CBR1 V88 ($p = 0.370$). In contrast, CBR1 V88 presented a 1.3-fold higher V_{max} for menadione than did CBR1 I88 ($p = 0.023$; Table 3). Consequently, CBR1 V88 showed a 1.3-fold higher turnover number (K_{cat}) for menadione. On the other hand, CBR1 V88 and CBR1 I88 K_m values for the substrates PGE_2 and daunorubicin did not differ significantly (PGE_2, $p = 0.234$; and daunorubicin, $p = 0.287$; Table 3). However, the maximal velocities of CBR1 V88 and CBR1 I88 for PGE_2 and daunorubicin differed significantly (PGE_2, $p < 0.01$; and daunorubicin, $p < 0.05$; Table 3; Fig. 2). On average, the V_{max} of CBR1 V88 was 51% (PGE_2) and 50% (daunorubicin) higher than the V_{max} of CBR1 I88. Consequently, CBR1 V88 showed increased turnover values for both PGE_2 (1.4- fold) and daunorubicin (1.5-fold) (Table 3). To further confirm the kinetic differences, we measured the amount of the C-13 alcohol metabolite daunorubicinol synthesized by CBR1 V88 and CBR1 I88. Under V_{max} conditions, CBR1 V88 synthesized 47% more daunorubicinol than did CBR1 I88 per unit of time ($p < 0.0001$; Fig. 3).

Kinetic studies with varying concentrations of NADPH (range 10–200 μM) and menadione (250 μM) showed a relatively lower K_m ($p = 0.095$) and a higher V_{max} ($p = 0.096$) for CBR1 V88 as compared with CBR1 I88 (Table 3). Further comparison of CBR1 V88 and CBR1 I88 data sets showed that the overall Michaelis-Menten kinetics for NADPH in the presence of menadione differed significantly between both isoforms ($p < 0.001$).

CBR1 V88 and CBR1 I88 Inhibition by Rutin

The development of specific CBR inhibitors has been proposed as a potentially useful therapeutic strategy to minimize the incidence of anthracycline-related cardiotoxicity during cancer treatment (Olson et al., 2003). Some flavonoids such as rutin, quercetin, and kaempferol inhibit CBR1 activity with IC_{50} values in the micromolar range (Wermuth, 1981). Therefore, we tested whether the CBR1 V88 and CBR1 I88 isoforms were distinctively inhibited by rutin. CBR1 V88 and CBR1 I88 displayed different levels of dose-dependent inhibition by rutin (Fig. 4). Interestingly, the rutin IC_{50} value for CBR1 I88 was 3.6-fold lower than the IC_{50} value obtained for CBR1 V88 (CBR1 I88 $IC_{50} = 15.0 \pm 0.1$ μM versus CBR1 V88 $IC_{50} = 54.0 \pm 0.4$ μM, $p < 0.001$).

CBR1 V88 and CBR1 I88 Thermolability

Some functional SNPs result in protein isoforms that show differential activity profiles after heat treatment (Yamada et al., 2001; Li et al., 2005). Consequently, we analyzed the thermolability of CBR1 V88 and CBR1 I88 by determining enzymatic activities at different temperatures with the substrates menadione and daunorubicin. CBR1 V88 and CBR I88 retained 100% of activity after heating to 46°C. Incubations at 50°C resulted in similar

reductions (≈13%) on the activities of CBR1 V88 and CBR1 I88. Both isoforms were rendered inactive after heating to 60°C (Fig. 5). In conclusion, CBR1 V88 and CBR1 I88 showed similar thermolability profiles.

CBR1 V88 and CBR1 I88 NADPH Binding Affinities

We performed isothermal titration calorimetric analyses to further explore the basis of the distinctive catalytic properties of CBR1 V88 and CBR1 I88. The NADPH titration profiles of CBR1 V88 and CBR1 I88 differed significantly ($p < 0.001$; Fig. 6, A and B). Further integration analyses demonstrated that both isoforms presented essentially identical values for enthalpy (ΔH), free Gibbs' energy (ΔG), and entropy (ΔS), respectively (Fig. 6, C and D; Table 4). Notably, CBR1 V88 and CBR1 I88 showed different NADPH dissociation constants (K_d; Table 4). The K_d of CBR1 I88 was 1.7-fold higher than the K_d of CBR1 V88. Therefore, the valine-to-isoleucine substitution encoded by the variant *CBR1* I88 allele results in a CBR1 isoform (I88) with lower affinity for the NADPH cofactor compared with the "wild-type" protein (V88).

Docking and Modeling Analysis

A three-dimensional atomic model of the polymorphic human CBR1-NADP-PGE_2 ternary complex was generated by docking a substrate molecule to the active site using the crystal structure of the human CBR1-NADP complex (Tanaka et al., 2005). Figure 7 is a close-up view of the active site showing the bound NADP molecule (pink), the docked substrate PGE_2 (yellow), and the location of the polymorphic V88I site. The polymorphic V88I site is situated behind the NADP molecule. The catalytic residues Y194, K198, and S140 are shown in blue. The I88 side chain has no direct contact either with NADP (distance ~9 Å) or with PGE_2. In the docked orientation, the $^{9}C{=}O$ group of PGE_2 makes a hydrogen bond with the catalytic Y194 side chain in the correct stereochemical orientation for the hydride and proton transfer for the reduction of PGE_2 to $PGE_{2\alpha}$ (with a $H^{9\alpha}C{-}OH$ functional group). Furthermore, this orientation of the $^{9}C{=}O$ group satisfies the mechanistic requirement that the direction of approach of the Pro-*S* hydride (from the ^{4}C position of the reduced nicotinamide ring) is roughly normal to the carbonyl plane. The carboxylic moiety of PGE_2 makes a salt bridge with the R145 side chain, an interaction that may be important for binding and stabilization of the substrate.

Discussion

Human CBR1 catalyzes the reduction of a wide variety of endogenous and xenobiotic compounds including the fever mediator PGE_2 and the anticancer anthracycline daunorubicin. CBR activity varies widely among individuals, and the reasons for such disparities remain to be elucidated. It is possible that genetic polymorphism may in part dictate variable CBR activity. Therefore, we conducted this study to identify and characterize the functional impact of SNPs in the coding region of *CBR1*. We detected three synonymous SNPs and one non-synonymous SNP on *CBR1* (*CBR1* V88I).

Our functional characterization studies with prototypical CBR1 substrates showed that *CBR1* V88I encodes for CBR1 isoforms with distinctive kinetic and thermodynamic properties. Interestingly, the CBR1 V88 isoform presented higher V_{max} values for PGE_2 (51%) and daunorubicin (50%) than did CBR1 I88. In agreement, CBR1 V88 synthesized higher levels (47%) of the cardiotoxic C-13 alcohol metabolite daunorubicinol than did CBR1 I88. Olson et al. (2003) reported that the plasma levels of C-13 alcohol metabolites 4 h after the administration of doxorubicin (20 mg/kg i.p.) were 75% higher in mice with two active *Cbr1* alleles (*Cbr1*+/+) than in heterozygous *Cbr1*+/− animals. The authors also observed that the overall 40 to 50% decrease in *Cbr1* protein levels among *Cbr1*+/− mice was sufficient to confer significant protection against anthracycline-related cardiotoxicity. As a result, the

percentages of dead animals 18 days after doxorubicin treatment were 91% (*Cbr1*+/+) versus 18% (*Cbr1*+/−). In this context, it is tempting to speculate that individuals with homozygous *CBR1* I88 genotype may exhibit a slower rate of synthesis of C-13 alcohol metabolites that may consequently have an impact on the risk of cardiotoxicity associated with the use of anthracyclines for cancer therapy.

CBR1 V88 also showed higher V_{max} (31%) for the small quinone substrate menadione (vitamin K_3), as compared with CBR1 I88. Together, our results suggest that the functional impact of *CBR1* V88I appears not to be substrate-specific. Therefore, it is possible that CBR1 V88 and CBR1 I88 would also differ in their ability to catalyze the reduction of other relevant CBR1 substrates such as the antipsychotic haloperidol or the potent carcinogen *N*-methyl-*N*-(4-oxo-4-pyridin-3-yl-butyl)nitrous amide (Someya et al., 1992; Kudo and Ishizaki, 1999; Forrest and Gonzalez, 2000).

CBR1 V88 and CBR1 I88 showed different Michaelis-Menten kinetics for the NADPH cofactor in the presence of the substrate menadione. In line with this finding, our titration calorimetry studies indicated that the NADPH dissociation constants (K_d) of CBR1 V88 and CBR1 I88 differed significantly (CBR1 V88 = 3.8 ± 0.5 μM versus CBR1 I88 = 6.3 ± 0.6 μM). Thus, the distinct catalytic activities of CBR1 V88 and CBR1 I88 toward different substrates are due to the fact that both isoforms bind the NADPH cofactor with different affinities. We performed molecular modeling together with substrate docking simulation using the crystal structure of human CBR1 to further define the molecular basis underlying the functional impact of CBR1 V88I. The docking of a PGE_2 molecule in the active site provided additional insights into the enzyme-substrate interplays during the catalytic reduction of PGE_2 by CBR1, in spatial relation to the V88I substitution. Figure 7 shows the CBR1-PGE_2 complex at the enzyme's active site. The model indicates that the ^{9}C=O group of PGE_2 accepts a proton from the Y194 hydroxyl group in a precise stereochemical orientation that allows the hydride and proton transfer during the reduction of the substrate. The ^{1}C carboxyl group of PGE_2 binds to the side chain of R145 through a salt bridge that stabilizes the enzyme-substrate complex during catalysis. The side chains inside and bordering the substrate, and cofactor-binding cavities including the catalytic residues K198, S194, and Y140 interact directly with NADP and the substrate (PGE_2). The model also shows that the V88I substitution is located behind the ribose moiety of the NADP molecule, roughly 9 Å away from it. At this polymorphic site, V88 packs against I20 in a hydrophobic pocket with restricted although sufficient space to accommodate the extra methyl group from variant I88. The methyl group from I88 increases the nonpolar surface area (V, 135 Å^2 versus I, 155 Å^2), and augments the overall hydrophobicity of the pocket. Thus, the altered packing between I20 and I88 may in turn have an impact on NADPH binding due to the proximity of the cofactor. This effect is probably reflected in the docking simulation result showing that the ternary CBR1-NADP-PGE_2 structure with the V88 side chain is energetically more favorable (−5.9 kcal/mol) than that with I88 (−3.6 kcal/mol). Together, these facts provide the structural rationale for the experimental differences between the NADPH dissociation constants of both isoforms.

Our genotypic survey suggests that the *CBR1* V88I polymorphism may be confined to individuals with African ancestry. Africa is the continent with the highest incidence of malaria and, for example, in Uganda, the number of cases per 1000 individuals is as high as 478 (http://www.globalhealthfacts.org). Recent studies suggest that elevated plasma levels of PGE_2 in healthy children infected with malarial parasites may protect against severe clinical forms of malaria (Perkins et al., 2001, 2005). In humans, malaria is the most powerful known source of genetic selective pressure, and the frequency of polymorphic changes with malaria-protective effects is expected to be higher in affected populations (Kwiatkowski, 2005). Therefore, we hypothesize that *CBR1* V88I may constitute a protective polymorphism against severe malaria because the slower CBR1 I88 isoform would result in higher levels of PGE_2

among carriers of the variant *CBR1* I88 allele. Genetic association studies on selected human groups are needed to test this hypothesis. In conclusion, we have identified and characterized the first genetic determinant of human CBR1 activity.

Acknowledgements

The excellent assistance of Jennifer Griswold and Darowan Akajagbor is gratefully acknowledged.

This work was supported by National Institutes of Health/National Institute of General Medical Sciences Grant R01GM73646 to J.G.B., and by National Institutes of Health/National Institute of General Medical Sciences Grant U01GM61393 and National Institutes of Health/National Institute of General Medical Sciences Pharmacogenetics Research Network and Database Grant U01GM61374 (http://pharmgkb.org). V.G.-C. is a Merck fellow.

ABBREVIATIONS

CBR
carbonyl reductase

SNP
single nucleotide polymorphism

PCR
polymerase chain reaction

PGE_2
prostaglandin E_2

HPLC
high-performance liquid chromatography

References

Bohren KM, von Wartburg JP, Wermuth B. Kinetics of carbonyl reductase from human brain. Biochem J 1987;244:165–171. [PubMed: 3311025]

Covarrubias VG, Lakhman SS, Forrest A, Relling MV, Blanco JG. Higher activity of polymorphic NAD (P)H:quinone oxidoreductase in liver cytosols from blacks compared to whites. Toxicol Lett 2006;164:249–258. [PubMed: 16478651]

Cowens JW, Creaven PJ, Greco WR, Brenner DE, Tung Y, Ostro M, Pilkiewicz F, Ginsberg R, Petrelli N. Initial clinical (phase I) trial of TLC D-99 (doxorubicin encapsulated in liposomes). Cancer Res 1993;53:2796–2802. [PubMed: 8504422]

Forrest GL, Gonzalez B. Carbonyl reductase. Chem-Biol Interact 2000;129:21–40. [PubMed: 11154733]

Forrest GL, Gonzalez B, Tseng W, Li X, Mann J. Human carbonyl reductase overexpression in the heart advances the development of doxorubicin-induced cardiotoxicity in transgenic mice. Cancer Res 2000;60:5158–5164. [PubMed: 11016643]

Ivanov AI, Romanovsky AA. Prostaglandin E2 as a mediator of fever: synthesis and catabolism. Front Biosci 2004;9:1977–1993. [PubMed: 14977603]

Ivanov AI, Scheck AC, Romanovsky AA. Expression of genes controlling transport and catabolism of prostaglandin E2 in lipopolysaccharide fever. Am J Physiol 2003;284:R698–R706.

Kruglyak L, Nickerson DA. Variation is the spice of life. Nat Genet 2001;27:234–236. [PubMed: 11242096]

Kudo S, Ishizaki T. Pharmacokinetics of haloperidol: an update. Clin Pharmacokinet 1999;37:435–456. [PubMed: 10628896]

Kwiatkowski DP. How malaria has affected the human genome and what human genetics can teach us about malaria. Am J Hum Genet 2005;77:171–192. [PubMed: 16001361]

Lakhman SS, Ghosh D, Blanco JG. Functional significance of a natural allelic variant of human carbonyl reductase 3 (*CBR3*). Drug Metab Dispos 2005;33:254–257. [PubMed: 15537833]

Li Y, Yang X, van Breemen RB, Bolton JL. Characterization of two new variants of human catechol O-methyltransferase in vitro. Cancer Lett 2005;230:81–89. [PubMed: 16253764]

Minotti G, Menna P, Salvatorelli E, Cairo G, Gianni L. Anthracyclines: molecular advances and pharmacologic developments in antitumor activity and cardiotoxicity. Pharmacol Rev 2004;56:185–229. [PubMed: 15169927]

Mordente A, Meucci E, Martorana GE, Giardina B, Minotti G. Human heart cytosolic reductases and anthracycline cardiotoxicity. IUBMB Life 2001;52:83–88. [PubMed: 11795600]

Nickerson DA, Tobe VO, Taylor SL. PolyPhred: automating the detection and genotyping of single nucleotide substitutions using fluorescence-based resequencing. Nucleic Acids Res 1997;25:2745–2751. [PubMed: 9207020]

Ohara H, Miyabe Y, Deyashiki Y, Matsuura K, Hara A. Reduction of drug ketones by dihydrodiol dehydrogenases, carbonyl reductase and aldehyde reductase of human liver. Biochem Pharmacol 1995;50:221–227. [PubMed: 7632166]

Olson LE, Bedja D, Alvey SJ, Cardounel AJ, Gabrielson KL, Reeves RH. Protection from doxorubicin-induced cardiac toxicity in mice with a null allele of carbonyl reductase 1. Cancer Res 2003;63:6602–6606. [PubMed: 14583452]

Perkins DJ, Hittner JB, Mwaikambo ED, Granger DL, Weinberg JB, Anstey NM. Impaired systemic production of prostaglandin E2 in children with cerebral malaria. J Infect Dis 2005;191:1548–1557. [PubMed: 15809915]

Perkins DJ, Kremsner PG, Weinberg JB. Inverse relationship of plasma prostaglandin E2 and blood mononuclear cell cyclooxygenase-2 with disease severity in children with Plasmodium falciparum malaria. J Infect Dis 2001;183:113–118. [PubMed: 11076710]

Pey AL, Martinez A. The activity of wild-type and mutant phenylalanine hydroxylase and its regulation by phenylalanine and tetrahydrobiopterin at physiological and pathological concentrations: an isothermal titration calorimetry study. Mol Genet Metab 2005;86(Suppl 1):S43–S53. [PubMed: 15936235]

Rosemond MJ, Walsh JS. Human carbonyl reduction pathways and a strategy for their study in vitro. Drug Metab Rev 2004;36:335–361. [PubMed: 15237858]

Someya T, Shibasaki M, Noguchi T, Takahashi S, Inaba T. Haloperidol metabolism in psychiatric patients: importance of glucuronidation and carbonyl reduction. J Clin Psychopharmacol 1992;12:169–174. [PubMed: 1629382]

Tanaka M, Bateman R, Rauh D, Vaisberg E, Ramachandani S, Zhang C, Hansen KC, Burlingame AL, Trautman JK, Shokat KM, et al. An unbiased cell morphology-based screen for new, biologically active small molecules. PLoS Biol 2005;3:e128. [PubMed: 15799708]

Weisberg IS, Jacques PF, Selhub J, Bostom AG, Chen Z, Curtis Ellison R, Eckfeldt JH, Rozen R. The 1298A→C polymorphism in methylenetetrahydrofolate reductase (MTHFR): in vitro expression and association with homocysteine. Atherosclerosis 2001;156:409–415. [PubMed: 11395038]

Wermuth B. Purification and properties of an NADPH-dependent carbonyl reductase from human brain. Relationship to prostaglandin 9-ketoreductase and xenobiotic ketone reductase. J Biol Chem 1981;256:1206–1213. [PubMed: 7005231]

Wermuth B, Platts KL, Seidel A, Oesch F. Carbonyl reductase provides the enzymatic basis of quinone detoxication in man. Biochem Pharmacol 1986;35:1277–1282. [PubMed: 3083821]

Wouters KA, Kremer LC, Miller TL, Herman EH, Lipshultz SE. Protecting against anthracycline-induced myocardial damage: a review of the most promising strategies. Br J Haematol 2005;131:561–578. [PubMed: 16351632]

Yamada K, Chen Z, Rozen R, Matthews RG. Effects of common polymorphisms on the properties of recombinant human methylenetetrahydrofolate reductase. Proc Natl Acad Sci USA 2001;98:14853–14858. [PubMed: 11742092]

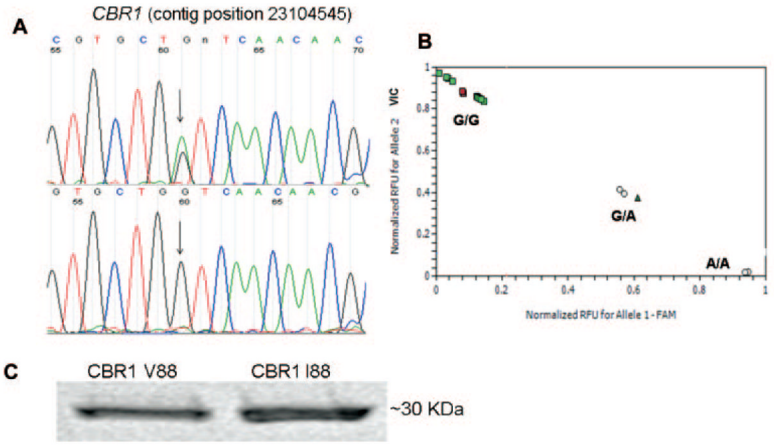

Fig. 1.

A, detection of *CBR1* V88I by DNA sequence analysis. The chromatogram at the top shows the sequence trace from an individual with heterozygous (G/A) genotype. The chromatogram at the bottom shows the trace from a subject with homozygous (G/G) genotype. B, *CBR1* V88I genotyping by real-time PCR. C, immunodetection of purified CBR1 V88 and CBR1 I88 with a specific anti-human CBR1 antibody.

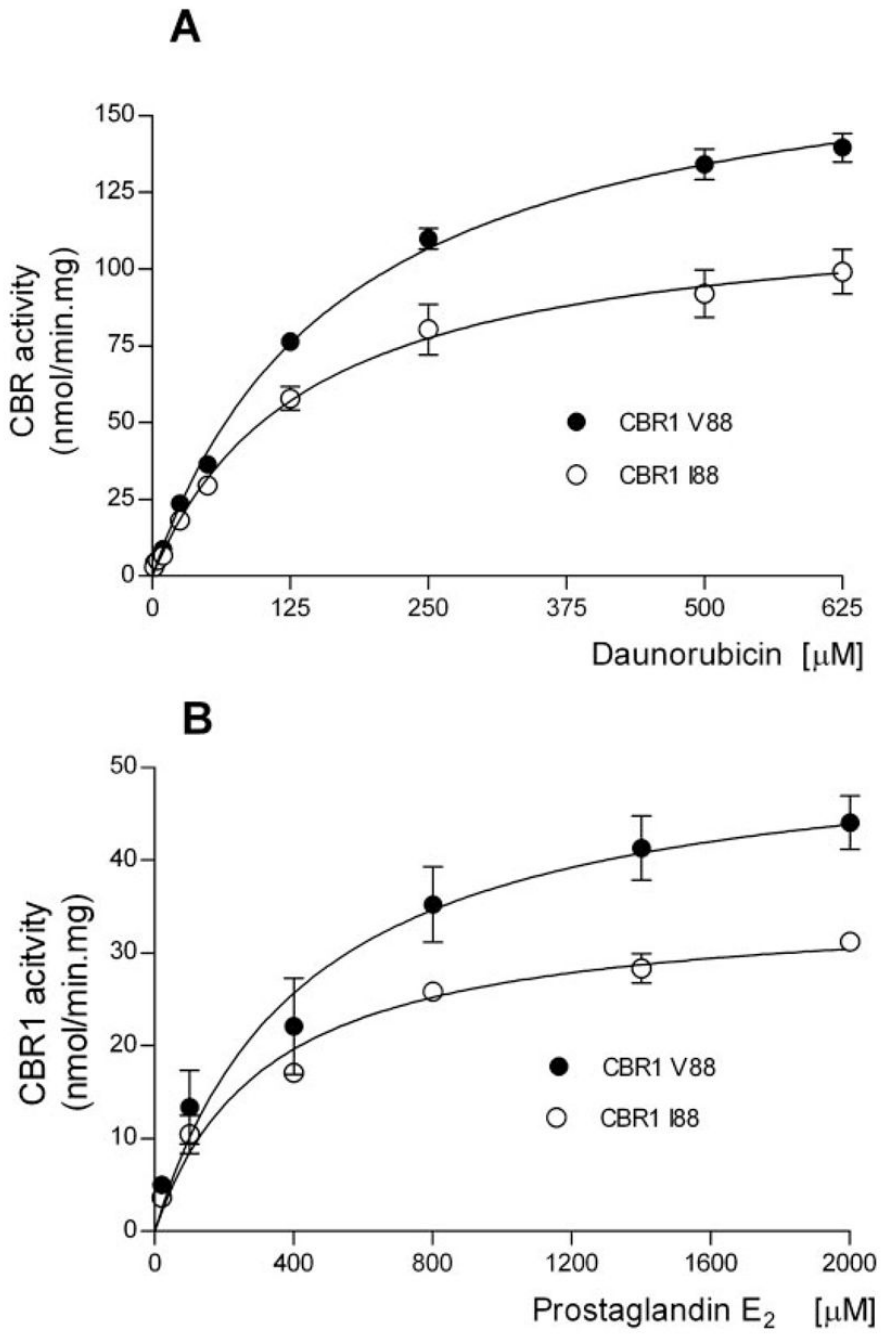

Fig. 2.

Kinetic characterization of CBR1 V88 and CBR1 I88 with the substrates daunorubicin (A) and prostaglandin E2 (B). Each point represents the mean ± S.D. of four experiments performed in duplicates with two independent protein preparations. Differences between curves were significant at $p < 0.05$ (A) and $p < 0.01$ (B).

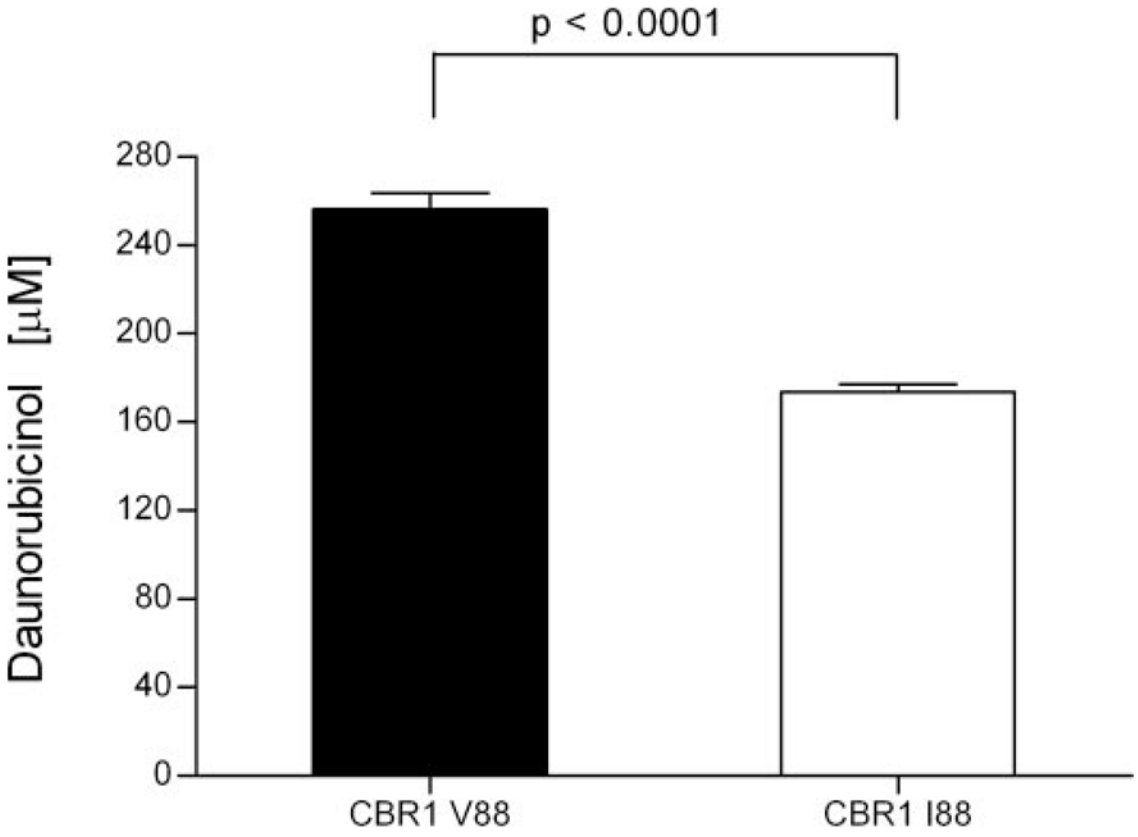

Fig. 3.
Synthesis of daunorubicinol by CBR1 V88 and CBR1 I88. Each bar represents the average ± S.D. of two independent experiments performed in duplicate.

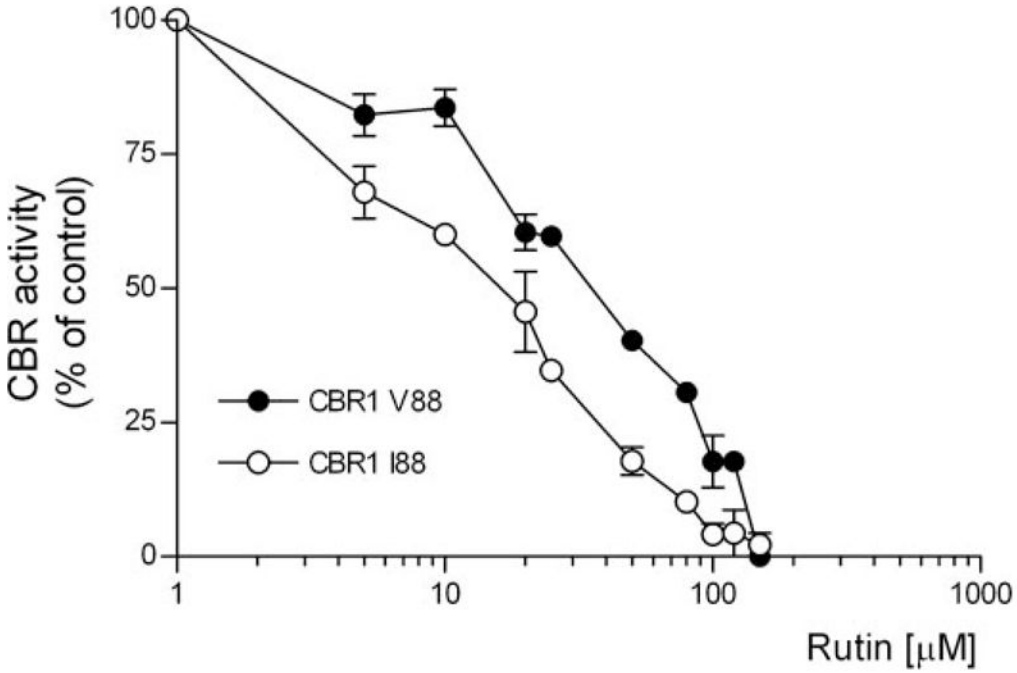

Fig. 4.

CBR1 V88 and CBR1 I88 inhibition by rutin (substrate = 40 μM menadione). Each point represents the average ± S.D. of two experiments performed in duplicate. Differences between inhibition curves were statistically significant at $p < 0.001$.

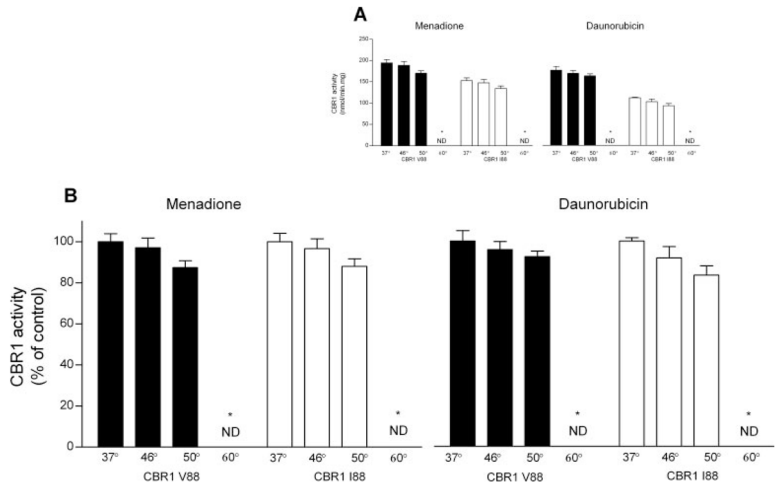

Fig. 5.

Thermolability profiles of CBR1 V88 and CBR1 I88. A, CBR1 V88 and CBR1 I88 maximal activities at different temperatures for the substrates menadione (left) and daunorubicin (right). B, CBR1 V88 and CBR1 I88 maximal activities relative to control incubations at 37°C (100%). Each value represents the average ± S.D. of two experiments performed in duplicate (ND, nondetectable).

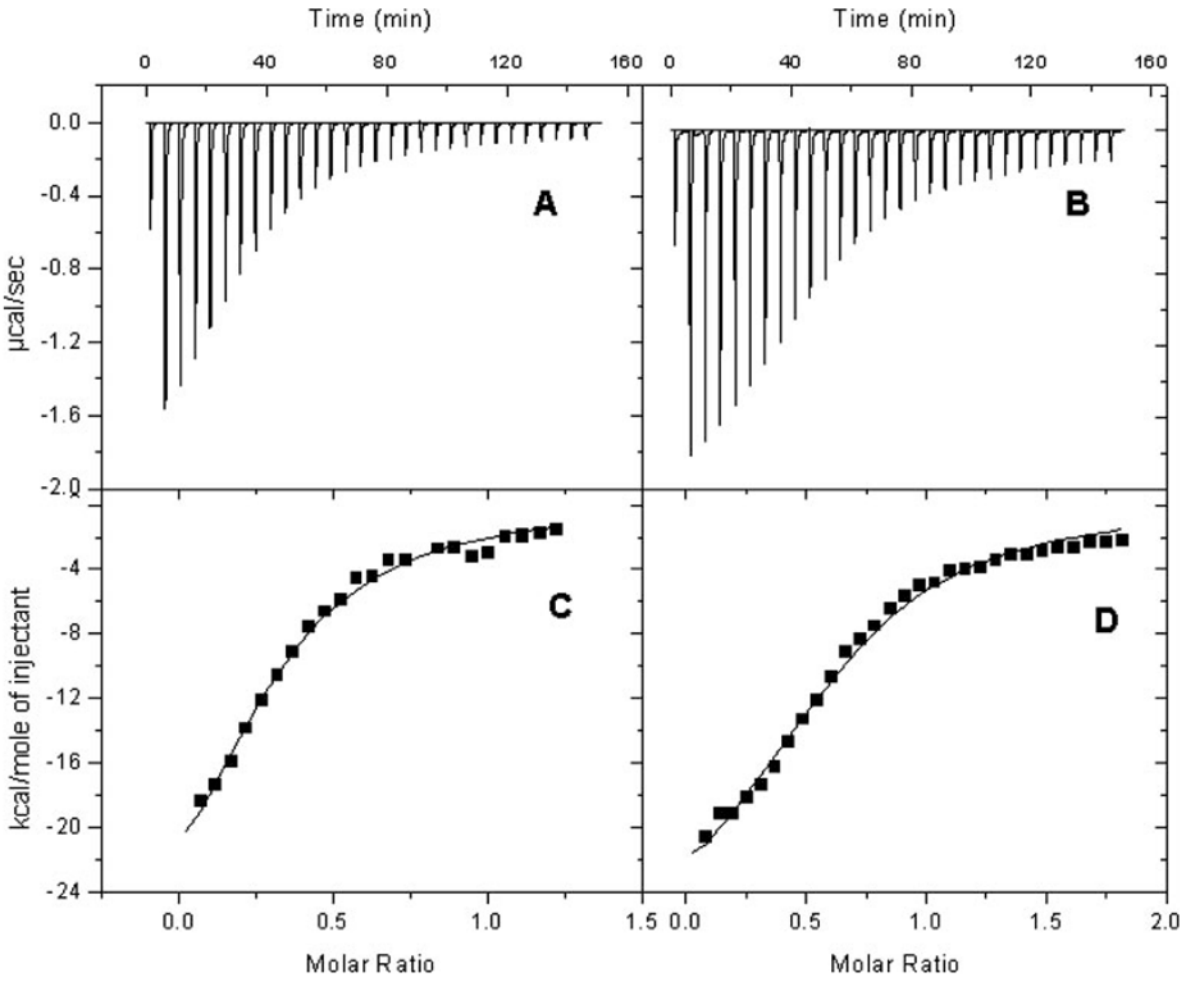

Fig. 6.

Isothermal titration calorimetry profiles of CBR1 V88 and CBR1 I88 with NADPH. Top, each peak shows the rate of heat release (μcal/s) after the interaction of CBR1 V88 (A) and CBR1 I88 (B) with the NADPH cofactor. Differences in titration profiles were significant at $p < 0.001$. Bottom, integration analysis for the titration profiles of CBR1 V88 (C) and CBR1 I88 (D). The solid line represents the best fit with a one-binding site model.

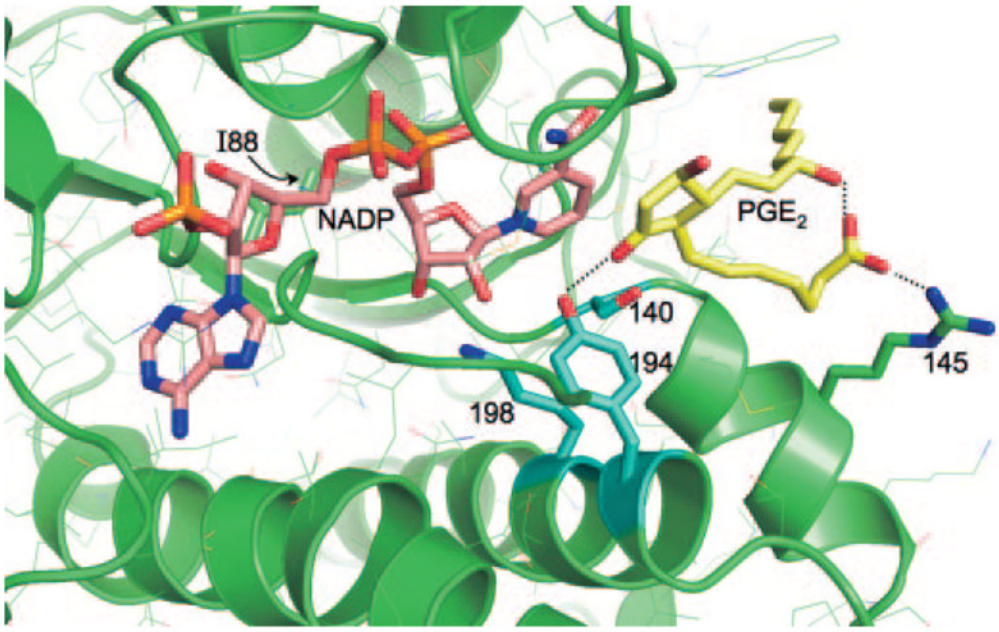

Fig. 7.

Three-dimensional model of the active site of polymorphic human CBR1 V88I with the substrate PGE_2. In this view, the polymorphic V88I residue is located behind the NADP molecule (pink). The catalytic residues Y194, K198, and S140 are shown in light blue, and PGE_2 is shown in yellow. Other side chains are shown in thin lines.

TABLE 1

Genotype distributions of common polymorphism in the coding region of CBR1

	N	L73L (G312C, rs25678)					A209A (C720T, rs20572)					V231V (G786A, rs2230192)				
		G/G	G/C	C/C	p	q	C/C	C/T	T/T	p	q	G/G	G/A	A/A	p	q
United States (European)	20	14	6	0	0.850	0.15	14	6	0	0.85	0.15	19	1	0	0.98	0.02
United States (African)	13	13	0	0	N.A.	N.A.	13	0	0	N.A.	N.A.	13	0	0	N.A.	N.A.

N.A., not applicable.

TABLE 2

CBR1 V88I genotype distribution in DNA human diversity panels

Population	*N*	G/G	G/A	A/A	*p*	*q*
United States (African)	70	68	2	0	0.986	0.014
United States (European)	50	50	0	0	N.A.	N.A.
Indo-Pakistani	9	9	0	0	N.A.	N.A.
Middle Eastern	10	10	0	0	N.A.	N.A.
Africans north of the Sahara	7	7	0	0	N.A.	N.A.
Africans south of the Sahara	9	9	0	0	N.A.	N.A.
Chinese	10	10	0	0	N.A.	N.A.
Japanese	10	10	0	0	N.A.	N.A.
Mexican	10	10	0	0	N.A.	N.A.
Asia Pacific	7	7	0	0	N.A.	N.A.
South American Andes	10	10	0	0	N.A.	N.A.
Southeast Asia	9	9	0	0	N.A.	N.A.

N, number of DNA samples from nonrelated individuals. *p* denotes the G allele, and *q* denotes the A allele, N.A. not applicable.

TABLE 3

CBR1 V88 and CBR1 I88 kinetic constants for prototypical substrates

Substrate	CBR1 V88				CBR1 I88			
	K_m	V_{max}	K_{cat}	V_{max}/K_m	K_m	V_{max}	K_{cat}	V_{max}/K_m
	μM	nmol/min · mg	S^{-1}	mg/min × 10^{-3}	μM	nmol/min · mg	s^{-1}	mg/min × 10^{-3}
Menadione[a]	42 ± 23	220 ± 27	110	5.20	55 ± 21	168 ± 16	85	3.06
Daunorubicin[a]	173 ± 26	181 ± 13	91	1.04	140 ± 23	121 ± 12	61	0.90
PGE_2[a]	309 ± 94	53 ± 7	25	0.17	320 ± 63	35 ± 4	18	0.11
NADPH[b]	247 ± 29	356 ± 30	179	1.44	343 ± 63	295 ± 31	149	0.86

[a] Values represent the mean ± S.D. from four experiments performed in duplicates with two independent protein preparations.

[b] Menadione was held constant at 250 μM. Values represent the mean ± S.D. from two experiments performed in duplicates with two independent protein preparations.

TABLE 4

Thermodynamic constants of CBR1 V88 and CBR1 I88 derived from microcalorimetry titration analyses with NADPH

	CBR1 V88	CBR1 I88
K_d[a] (μM)	3.8 ± 0.5	6.3 ± 0.6
K_a[a] × 10^5 M^{-1}	2.6 ± 0.2	1.6 ± 0.2
ΔH (kcal/mol)	−29 ± 1	−29 ± 1
ΔG (kcal/mol)	−52 ± 1	−51 ± 1
$T\Delta S$ (kcal/mol)	−20 ± 1	−21 ± 1

[a]Differences between CBR1 variant isoforms were significant at $p < 0.001$.